Full length article

Proteomic and metabolomic responses in D-shape larval mussels *Mytilus galloprovincialis* exposed to cadmium and arsenic

CrossMark

Huifeng Wu [a], [*], Lanlan Xu [a], [b], Chenglong Ji [a], Deliang Yu [a], [b]

[a] *Key Laboratory of Coastal Zone Environmental Processes, Yantai Institute of Coastal Zone Research (YIC), Chinese Academy of Sciences (CAS), Shandong Provincial Key Laboratory of Coastal Zone Environmental Processes, YICCAS, Yantai 264003, PR China*
[b] *University of Chinese Academy of Sciences, Beijing 100049, PR China*

ABSTRACT

Cadmium (Cd) and arsenic (As) are the main metal/metalloid contaminants in the coastal environments of the Bohai Sea, China. In this work, a combined proteomic and metabolomic approach was applied to investigate the biological effects of Cd and As (V) in the early life stage (D-shape larvae) of mussel *Mytilus galloprovincialis*. Results indicated that Cd was a potential immune toxicant to D-shape larval mussel because of the numerous proteomic responses related to immune system. Additionally, Cd induced oxidative stress, cellular injury and disturbance in nucleic acid metabolism in D-shape larval mussels. However, only two identified proteins were significantly altered in As (V)-treated group, suggesting that D-shape larval mussel was less sensitive to As (V) than to Cd at protein level. These two proteins in response to As (V) suggested that As (V) influenced anti-oxidative system and cell proliferation in D-shape larval mussels. Metabolic responses indicated that Cd and As (V) induced disturbances in osmotic regulation and energy metabolism in D-shape larval mussels via different metabolic pathways. In addition, Cd reduced lipid metabolism as well. This work demonstrated that a combination of proteomics and metabolomics could provide an insightful view in the biological effects of pollutants in mussel *M. galloprovincialis* at an early life stage.

© 2016 Published by Elsevier Ltd.

1. Introduction

As it is known, there are numerous metal (e.g., zinc, gold) mining and smelting factories along the Bohai coast, which has led to severe metal pollution in the Bohai marine and coastal environments. Mu et al. (2009) found that Cd and As were the dominant metal pollutants in the sediments from the Laizhou Bay [1]. In the mussels collected from the Bohai Sea in China, a survey reported that the mussels from some of the sampling sites were polluted by Cd and As with average concentrations at ~2 and 5 μg/L, respectively [2]. In our recent study, the Cd and As pollution have been confirmed by the high accumulations of Cd and As in marine shrimp *Crangon affinis* collected from the Yellow River Estuary and Laizhou Bay along the Bohai coast, respectively [3]. Although Cd is relatively rare in marine environment, the concentration of Cd has reached 50 μg/L in some heavily polluted estuaries or harbors and ports [4]. In open ocean seawater, the concentration of total arsenic

is usually around 1 μg/L and As (V) is the dominant form of inorganic arsenic [5].

Both Cd and As are known carcinogens and environmental toxicants inducing multiple toxicities in animals. Cd may inactivate many metabolic enzymes by competing for the catalytic sites with other metals [6,7]. In addition, both Cd and As can induce oxidative stress in animals by producing excessive reactive oxygen species [8]. Since Cd and As have become severe metal/metalloid contaminants in the Bohai coast, it is necessary to characterize the biological effects of Cd and As in marine animals.

As two main -omic approaches in system biology, proteomics and metabolomics, have been well-established and successfully applied in marine biology [9,10]. Since proteomics and metabolomics can directly characterize the minor metabolite and protein responses, these two −omic techniques and their combination have represented their practicability to elucidate the biological effects and mechanisms of pollutants in environmental bioindicators. Especially, a combination of proteomics and metabolomics could validate and complement one another, when testing the biological effects of environmental pollutants [11,12].

Marine mussels are widely used as bioindicators in

* Corresponding author.
  E-mail address: hfwu@yic.ac.cn (H. Wu).

environmental monitoring and assessment programs because of their sessile filter, feeding lifestyle and high accumulation for organic and inorganic pollutants in the marine environment [13]. Usually, the adult mussels are applied in either ecotoxicology or environmental monitoring programs. Due to the immature defense system, however, the early life stages of animals are more sensitive than adults, which may present differential responsive profiles to environmental pollutants [14]. To our knowledge, the responses of early life stages of mussels under Cd and As (V) stresses were not fully characterized. Consequently, it is necessary to elucidate the biological effects and responsive mechanisms in the early life stage of mussel exposed to the environmentally relevant concentration of Cd and As (V). In this work, we planned to use the early life stage, D-shape larval mussel *M. galloprovincialis*, as the experimental animal to elucidate the biological effects of Cd and As at an environmentally relevant concentration (5 μg/L). Both two-dimensional gel electrophoresis (2-DE)-based proteomics and proton nuclear magnetic resonance (^{1}H NMR)-based metabolomics were conducted on the D-shape larval mussel samples to elucidate the biological effects of Cd and As (V) in the early life stage (D-shape larvae) of mussel *M. galloprovincialis*.

2. Materials and methods

2.1. Larvae breeding and experimental design

Adult mussels *M. galloprovincialis* reached sexual maturity were collected in April 2015 from a less disturbed site (Yantai, China). All mussels were transported to the laboratory and acclimatized in aerated natural seawater (salinity 31 psμ) at 21 °C for 7 days. After acclimatization, these mussels were kept in the air in dark place for 2 h. Then each mussel was put into a beaker containing warmer seawater (24 °C). After 2 h, the majority of mussels came to ovulation and spermiation. The 500 mesh sieve screen was used to filter impurities. Then the sperms and eggs were quickly collected to fertilize. All the fertilized eggs were then transferred into normal filtered seawater (50 L) in a bucket. Continuous aeration was conducted during incubation. After approximately 48 h, the majority of fertilized eggs developed into D-shape larvae (Fig. 1). Then the D-shape larval mussels were divided into three groups (control, Cd (as CdCl$_2$) and As (V) (as Na$_3$AsO$_4$) exposures) each containing 8 buckets (50 L) with a density of ~25 D-shape larval per milliliter. The environmentally relevant concentration (5 μg/L) of Cd and As was used for the exposures of D-shape larval mussels *M. galloprovincialis*. During the acclimatization and exposure
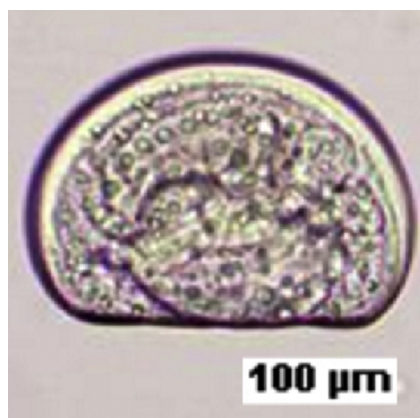

Fig. 1. A representative image of a D-shape larval mussel *M. galloprovincialis* from control group.

periods, all the D-shape larvae were kept under a photoperiod of 12 h light and 12 h dark, and fed with the *Chlorella vulgaris* daily. In control and treatment groups, all the D-shape larval mussels were not significantly different in morality and morphology. After exposure for 48 h, all the larvae (~1.0–1.3 × 10^6 individuals) from each bucket were immediately filtered out by 500 mesh sieve screen and collected into two larvae samples for proteomic and metabolomic analysis, respectively. These D-shape larval mussel samples were quickly snap-frozen in liquid nitrogen and stored at −80 °C.

2.2. Metabolite and protein extraction

Polar metabolites in D-shape larval mussels ($n = 8$ for each treatment) were extracted by the extraction protocol with some modifications [15]. All the D-shape larval mussel samples (ca. 100 mg wet weight) were homogenized and extracted in 4 mL/g of methanol, 5.25 mL/g of water and 2 mL/g of chloroform. The methanol/water layer with polar metabolites was transferred to a glass vial and then dried in a centrifugal concentrator. The extracts of soft tissue were then re-suspended in 600 μL of phosphate buffer (100 mM Na$_2$HPO$_4$ and NaH$_2$PO$_4$, including 0.5 mM TSP, pH 7.0) in D$_2$O. The mixture was vortexed and then centrifuged at 3000g for 5 min at 4 °C. The supernatant substance (550 μL) was then pipetted into a 5 mm NMR tube prior to NMR analysis.

Total protein extraction was performed based on previous studies with some modifications [16,17]. Briefly, each D-shape larval mussel samples was homogenized quickly on ice with 1 mL of TRIzol reagent and centrifuged at 12000g for 5 min at 4 °C. The supernatant was added with 200 μL of chloroform before shaking vigorously for 3 min and precipitating for 3 min, then the mixture was centrifuged at 12000g for 15 min at 4 °C, and its upper aqueous layer was discarded. A volume of 300 μL of absolute ethyl alcohol was added and the mixture was allowed to stand for 3 min at room temperature before being centrifuged at 2000g for 5 min at 4 °C. The phenol/ethanol supernatant was precipitated for 30 min at room temperature by the addition of 750 μL of isopropanol prior to centrifugation at 14000g for 10 min at 4 °C. Pellets obtained were washed with 1 mL of ethanol (v/v 95%) and centrifuged at 14000g for 10 min at 4 °C. This procedure was repeated twice. The pellets were solubilized in the lysis buffer (7 M urea; 2 M thiourea; 4% m/V CHAPS; 65 mM DTT and 0.2%W/V Bio-lyte buffer) and then incubated for 3 h at room temperature. The homogenate was centrifuged at 15000g for 10 min and the supernatant was applied to electrophoresis. The total concentrations of proteins were determined by Protein Assay Kit of TianGen.

2.3. ^{1}H NMR spectroscopy

Metabolite extracts of D-shape larval mussel samples were analyzed on a Bruker AV 500 NMR spectrometer performed at 500.18 MHz (at 25 °C) as described previously [18]. All ^{1}H NMR spectra were phased, baseline-corrected, and calibrated (TSP at 0.0 ppm) manually using TopSpin (version 2.1, Bruker).

2.4. Spectral pre-processing and multivariate analysis

All one dimensional ^{1}H NMR spectra were converted to a data matrix using the custom-written ProMetab software in Matlab version 7.0 (The MathsWorks, Natick, MA) [18]. Each spectrum was segmented into bins with a width of 0.005 ppm between 0.2 and 10.0 ppm. The bins of residual H$_2$O between 4.70 and 5.20 ppm were excluded from all the NMR spectra. The total spectral area of the remaining bins was normalized to unity to facilitate the comparison between the spectra. All the NMR spectra were generalized

log transformed (glog) with a transformation parameter $\lambda = 2.0 \times 10^{-9}$ to stabilize the variance across the spectral bins and to increase the weightings of the less intense peaks [18]. As described in details in our previous work, data were mean-centered before multivariate analysis [18]. Furthermore, the supervised multivariate data analysis methods, partial least squares discriminant analysis (PLS-DA) and orthogonal projection to latent structure with discriminant analysis (OPLS-DA), were sequentially carried out to uncover and extract the statistically significant metabolite variations related to Cd and As (V) exposures, as described previously. Metabolites were assigned following the tabulated chemical shifts and by using the software, Chenomx (Evaluation Version, Chenomx Inc., Edmonton, Alberta, Canada) [18].

2.5. Two-dimensional gel electrophoresis, image acquisition and data analysis

For the first dimension (IEF), 130 µg of protein was loaded onto IPG strips with a linear pH gradient from 4 to 7 (Immobiline Dry-strip TM 24 cm, GE Healthcare, USA) The isoelectric focusing gel solution (7 M urea, 2 M thiourea, 4% m/v CHAPS, 65 mM DTT, 0.001% m/v bromophenol blue and 0.2% W/V Bio-lyte buffer). IEF was conducted at 20 °C with an Ettan IPGphor3 system for a total of 85858 Vh (active rehydration was carried out at 30 V for 12 h, followed by 100 V for 5 h, 500 V for 1 h, 1000 V for 1 h, and a linear increase of voltage to 8000 V for 11 h and stand by 500 V for the second dimension).

After the first dimension, all the strips were placed in equilibration buffer (0.05 M Tris–HCl, pH 8.8; 6 M urea; 30% glycerol; 2% (w/v) SDS; containing 1% (w/v) DTT) and were slowly shaken for 15 min. The strips were then incubated for another 15 min in the equilibration buffer with 2.5% (w/v) iodoacetamide without DTT. The second dimension was conducted on 12.5% SDS-PAGE gels using the Ettan DALTsix system. After electrophoresis, the gels were silver stained by following the method of Mortz and Gharahdaghi [19,20]. Images were captured by ImageScanner III and spots were quantitatively analyzed using ImageMaster 2D Platinum 7.0. For all the matched spots, only protein spots with significant changes of at least 2.0 folds, and deemed significant by Student's t-test at a level of 95% were accepted as differentially expressed proteins.

2.6. In gel digestion and MS analysis

In gel digestion was performed according to Katayama et al. [21]. After being completely dried, the D-shape larval mussel samples were re-suspended with 5 µL of 0.1% TFA followed by mixing in 1:1 ratio with a saturated solution of α-cyano-4-hydroxy-trans-cinnamic acid in 50% acetonitrile [22]. One microliter of mixture was analyzed by an ABI 4800 MALDI-TOF/TOF Plus mass spectrometer (Applied Biosystems, Foster City, USA), data were acquired in a positive MS reflector using a CalMix5 standard to calibrate the instrument (ABI4800 Calibration Mixture). Both the MS and MS/MS data were integrated and processed using the GPS Explorer V3.6 software (Applied Biosystems, USA) with default parameters. Proteins were successfully identified based on 95% or higher confidence interval of their scores in the MASCOT V2.4 search engine (Matrix Science Ltd., London, U.K.). The following parameters were used in the search: NCBInr Metazoa (Animals) (2861494 sequences) database; trypsin as the digestion enzyme; one missed cleavage site; partial modifications of cysteine carbamidomethylation and methionine oxidization; no fixed modifications; 0.15 Da for precursor ion tolerance and 0.25 Da for fragment ion tolerance. Individual ions scores >40 indicate identity or extensive homology ($P < 0.05$).

3. Results and discussion

3.1. Proteomic responses in D-shape larval mussels exposed to Cd and As (V)

Proteomic responses related to Cd and As (V) exposures were determined by 2-DE-based proteomics in D-shape larval mussels, respectively (Fig. 2). Approximately, 1000 protein spots were resolved in the 2-DE gels from the D-shape larval mussel samples. A total of 17 spots resolved in 2-DE gels were differentially expressed (>2 folds, $P < 0.05$) in Cd and As (V) treatments. Fig. 2 shows the
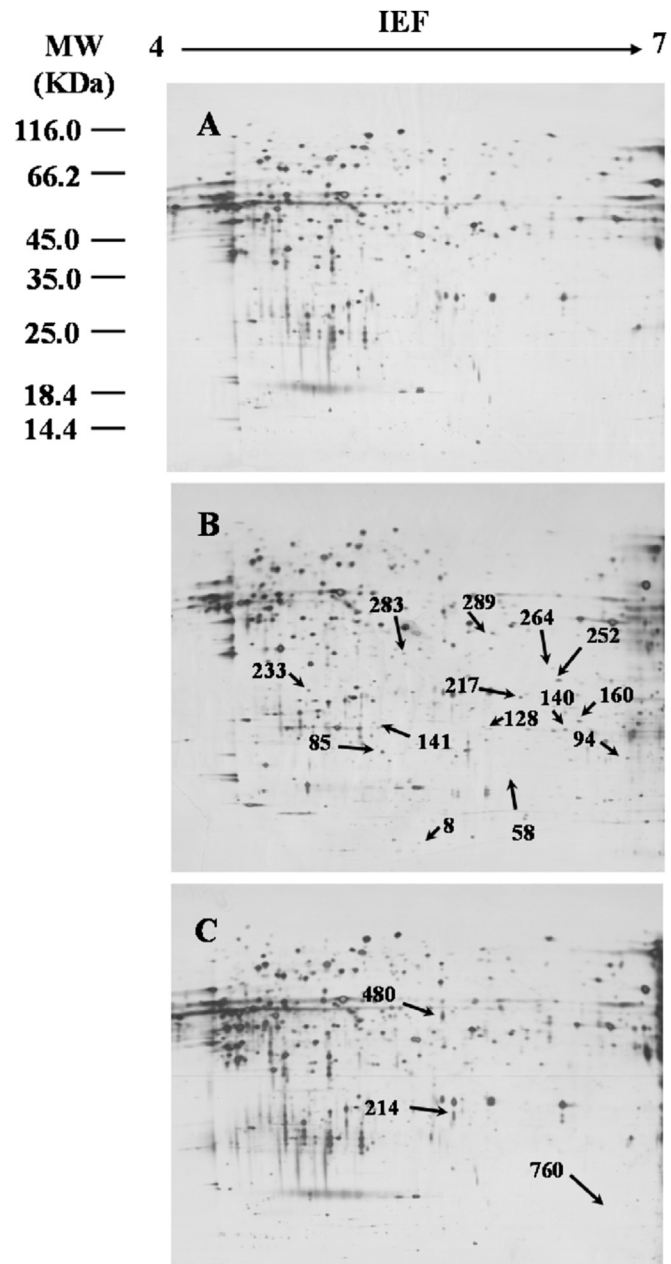

Fig. 2. Representative 2-D gels of proteins extracted from D-shape larval mussels *Mytilus galloprovincialis*. First dimension was performed using 130 µg of total soluble proteins on linear gradient IPG strips with pH 4–7. In the second dimension, 12.5% SDS-PAGE gels were used and proteins were visualized using silver staining. (A) control group, (B) Cd- and (C) As (V)-exposed group. Arrows show protein spots that changed significantly from inorganic As-exposed group compared to the control group.

differential protein spots in D-shape larval mussels exposed to Cd and As (V). All the differentially expressed proteins in all three biological replicates of silver-stained gels were analyzed by MALDI-TOF/TOF mass spectrometry and successfully identified. The information of these proteins is summarized in Table 1.

In Cd-exposed D-shape mussel samples, a total of 14 significantly differential spots were discovered, including 12 up-regulated and 2 down-regulated. These proteins were related to stress and defense (heat shock cognate 70, DnaJ-like protein, manganese superoxide dismutase and NADH dehydrogenase), protein homeostasis and proteolysis (peptidylprolyl isomerase protein, endoplasmic reticulum protein ERp 29 and four proteasome subunits), energy (malate dehydrogenase), skeleton (dynein light chain 1), nucleic acid metabolism (inorganic pyrophosphatase) and cell growth and development (deoxyribonucleoside 5'-monophosphate N-glycosidase).

Interestingly, only 3 differentially expressed proteins (2 up-regulated and 1 down-regulated) were observed in As (V)-exposed D-shape larval mussel samples, which might suggest that D-shape larval mussel was less sensitive to As (V) than to Cd with the environmentally relevant concentration (5 μg/L) at protein level. These altered proteins were basically involved in stress and defense (S-adenosylhomocysteine hydrolase) and cell growth and development (Ring box protein). One hypothetical protein was also found in As (V)-exposed D-shape larval mussel group.

As a stress protein in heat shock protein 70 family, heat shock cognate 70 is involved in immune system. It usually functions as a molecular chaperon and exerts important roles in folding of newly synthesized polypeptides, membrane translocation and degradation of misfolded proteins [23]. The DnaJ proteins, also known as heat shock protein 40, are proteins acting as co-chaperones to the molecular chaperone, heat shock protein 70 [24]. Endoplasmic reticulum protein ERp29 is a ubiquitously expressed endoplasmic reticulum stress-inducible protein that executes protective action by binding to denatured or aggregated cellular proteins thereby facilitating their refolding [25]. Proteasomes play a critical role in ubiquitin-mediated protein degradation through the ubiquitin−proteasome pathway and are involved in cell proliferation, apoptosis and stress responses [26]. He et al. found that the transcription of proteasome in hemocytes was up-regulated in *Penaeus japonicus* after microbial challenge [27]. Additionally, the up-regulated proteasome was also observed in bacteria-challenged mussel *M. galloprovincialis* [28]. Therefore proteasomes may function as an essential component in immune system in marine invertebrates. Interestingly, four proteasome subunits were highly significantly up-regulated in Cd-treated D-shape larval mussels. Therefore, the down-regulated heat shock cognate 70, up-regulated DnaJ-like protein, endoplasmic reticulum protein ERp29 and four proteasome subunits suggested that Cd exposure induced severe immune stress in D-shape larval mussels due to the immature immune system at this early life stage.

Manganese superoxide dismutase plays an important role in regulating cellular redox homeostasis by catalyzing the dismutation of superoxide into oxygen and hydrogen peroxide [29]. As a flavoprotein, NADH dehydrogenase processes iron-sulfur centers and is involved in production of reactive oxygen species in mitochondria [30]. Peptidylprolyl isomerase A is a known protein recognized as the marker of apoptosis that is also related to oxidative stress [31]. Therefore, the significant up-regulation of manganese superoxide dismutase, NADH dehydrogenase and peptidylprolyl isomerase A indicated the clear oxidative stress and consequent apoptosis induced by Cd in D-shape larval mussels. Malate dehydrogenase is a key metabolic enzyme in Krebs cycle that is related to energy metabolism. The up-regulated malate dehydrogenase implied the disturbance in energy metabolism induced by Cd in D-shape larval mussels. Moreover, malate dehydrogenase can also provide NADH for redox reaction. The up-regulation of malate dehydrogenase was therefore consistent with the up-regulation of NADH dehydrogenase, which is related to oxidative stress induced by Cd treatment in D-shape larval mussels. Dynein light chain 1 is an 8-kDa component of the cytoplasmic dynein complex that is a minus-end-directed microtubule-based motor [32]. The up-regulated dynein light chain meant the cellular injury induced by Cd in D-shape larval mussels.

Table 1
List of protein spots that differentially expressed in D-shape larval mussels *Mytilus galloprovincialis* exposed to Cd and As (V).

Spot ID[c]	Category and name	Species	gi number[d]	MW/kDa	PI	Protein score[e]	SC[f]	PN[g]	Fold change[h]
Stress and defense									
8	Heat shock cognate 70	*Mytilus galloprovincialis*	76780612	71.508	5.29	1098	25%	8	−2.16[a]
58	DnaJ-like protein subfamily B member 11	*Crassostrea gigas*	405965494	154.005	5.05	276	3%	3	2.80[a]
252	mitochondrial Manganese superoxide dismutase	*Mytilus galloprovincialis*	402122769	25.412	6.44	380	17%	2	4.89[a]
233	NADH dehydrogenase	*Crassostrea ariakensis*	405968356	18.778	5.06	94	16%	2	2.20[a]
760	S-adenosylhomocysteine hydrolase	*Crassostrea ariakensis*	253769244	48.182	5.97	62	2%	2	−2.24[b]
Protein homeostasis and proteolysis									
264	Peptidylprolyl isomerase protein, partial	*Crassostrea gigas*	163637061	14.731	5.29	58	6%	2	2.71[a]
128	Endoplasmic reticulum protein ERp29	*Crassostrea ariakensis*	405975720	28.444	5.19	51	6%	3	3.12[a]
140	Proteasome subunit alpha type-4	*Crassostrea ariakensis*	405964515	21.464	5.69	178	18%	3	7.51[a]
141	Proteasome subunit beta type-3	*Crassostrea gigas*	405971643	18.44	4.85	181	19%	2	2.66[a]
160	Proteasome subunit alpha type-6	*Crassostrea ariakensis*	405975869	25.429	7.57	153	10%	2	6.85[a]
217	Proteasome subunit alpha type-2	*Crassostrea ariakensis*	405964525	26.405	5.52	330	24%	4	10.55[a]
Energy									
94	Malate dehydrogenase	*Crassostrea ariakensis*	253769246	36.368	8.2	105	3%	2	2.51[a]
Skeleton									
289	Dynein light chain 1, axonemal, partial	*Crassostrea gigas*	405970124	21.189	5.53	61	15%	2	2.32[a]
Nucleic acid metabolism									
85	Inorganic pyrophosphatase	*Crassostrea gigas*	405962800	48.936	5.75	47	2%	1	2.30[a]
Cell growth and development									
283	Deoxyribonucleoside 5'-monophosphate N-glycosidase	*Crassostrea gigas*	405951747	15.878	5.18	40	5%	1	−2.72[a]
480	Ring box protein, partial	*Ostrea edulis*	387598207	13.646	5.27	47	6%	2	2.06[b]
Others									
214	Hypothetical protein CGI_10017570, partial	*Crassostrea gigas*	405973072	72.905	5.16	49	1%	1	2.12[b]

[a,b] Identification of differentially expressed proteins in D-shape larval mussel *M. galloprovincialis* exposed to Cd and As (V). [c] Assigned spot ID as indicated in Fig. 1. [d] gi numbers in NCBInr database. [e] Mascot score reported. [f] Sequence coverage. [g] Number of peptide sequences. [i] Fold changes with significant changes (>2.0 folds and $P < 0.05$) were calculated using ImageMaster 2D Platinum 7.0.

Inorganic pyrophosphatase catalyzes the reversible transfer of phosphoryl group from a polyphosphate to water and this reaction provides a thermodynamic pull for the synthesis of proteins and nucleic acids [33]. Deoxynucleoside 5'-monophosphate N-glycosidase catalyzes the hydrolysis of the N-glycosidic bond of the nucleotide to give deoxyribose 5-phosphate and a nucleobase, preferentially a purine [34]. The up-regulated inorganic pyrophosphatase and deoxynucleoside 5'-monophosphate N-glycosidase suggested the disturbance in nucleic acid metabolisms induced by Cd in D-shape larval mussels.

For As (V) treatment, only two identified proteins including S-adenosylhomocysteine hydrolase and ring box protein were significantly altered in D-shape larval mussels. It seemed that As (V) was less toxic than Cd to D-shape larval mussels. Due to its anion form (AsO_4^{3-}), As (V) is much less permeable than other cations of metals to the marine animals. Therefore, As (V) might be less toxic than Cd to D-shape larval mussels. S-adenosylhomocysteine hydrolase is a cytosolic enzyme that has important functions in the cytosolic metabolism linking processes of transmethylation, transsulfuration, and purine metabolism [35]. In a previous study, Company et al. (2011) pointed out that S-adenosylhomocysteine hydrolase was related to oxidative stress conditions and might be affected by reactive oxygen species-inducing stressors, including metals [35]. Obviously, the altered S-adenosylhomocysteine hydrolase implied that As (V) induced oxidative stress via different pathways compared with Cd exposure in D-shape larval mussels. Ring box protein is essential for cell proliferation and embryonic development in organisms [36]. The up-regulated ring box protein suggested that As (V) influenced cell proliferation in D-shape larval mussels.

3.2. Metabolomic responses in D-shape larval mussels exposed to Cd and As (V)

Fig. 3 shows the representative ^{1}H NMR spectra of extracts from D-shape larval mussels from control, Cd and As (V) treatments. A total of 31 metabolites were identified in D-shape larval mussel samples, including amino acids (valine, leucine, isoleucine, alanine, threonine, glycine, etc.), osmolytes (betaine, homarine, dimethylglycine, taurine and hypotaurine), intermediates in the Krebs cycle (succinate and fumarate) and energy metabolism-related metabolites (glucose, glycogen and ATP).

The supervised pattern recognition method, OPLS-DA, was performed on the NMR spectral data for metabolic biomarker discovery in Cd- and As (V)-treated mussel groups, respectively (Fig. 4). The scores plots indicated the robust separation between control and treatments with reliable Q^2 values (>0.6) (Fig. 4A and C). From the loading plot (Fig. 4B), the concentrations of alanine, glutamine, acetoacetate, succinate, hypotaurine and glycine were significantly ($P < 0.05$) decreased in Cd-treated D-shape larval mussel samples. However, the concentrations of aspartate and phosphocholine were significantly ($P < 0.05$) increased. Compared to the metabolic profile from Cd-treated group, several metabolites were similarly altered including alanine, acetoacetate, aspartate and phosphocholine in As (V)-treated group (Fig. 4D). However, elevated dimethylglycine and betaine and depleted β-alanine, malonate, glucose and glycogen were uniquely detected in As (V)-treated mussel samples.

Hypotaurine is a known osmolyte in marine bivalves. The free amino acids are usually involved in two main pathways including oxidation for energy production and osmoregulation [10]. In the Cd-treated group, the depleted hypotaurine, glutamine, glycine and alanine implied that Cd exposure disturbed osmotic regulation in D-shape larval mussels. In addition, alanine is also the major end product in the anaerobic breakdown of glucose in bivalves [37].
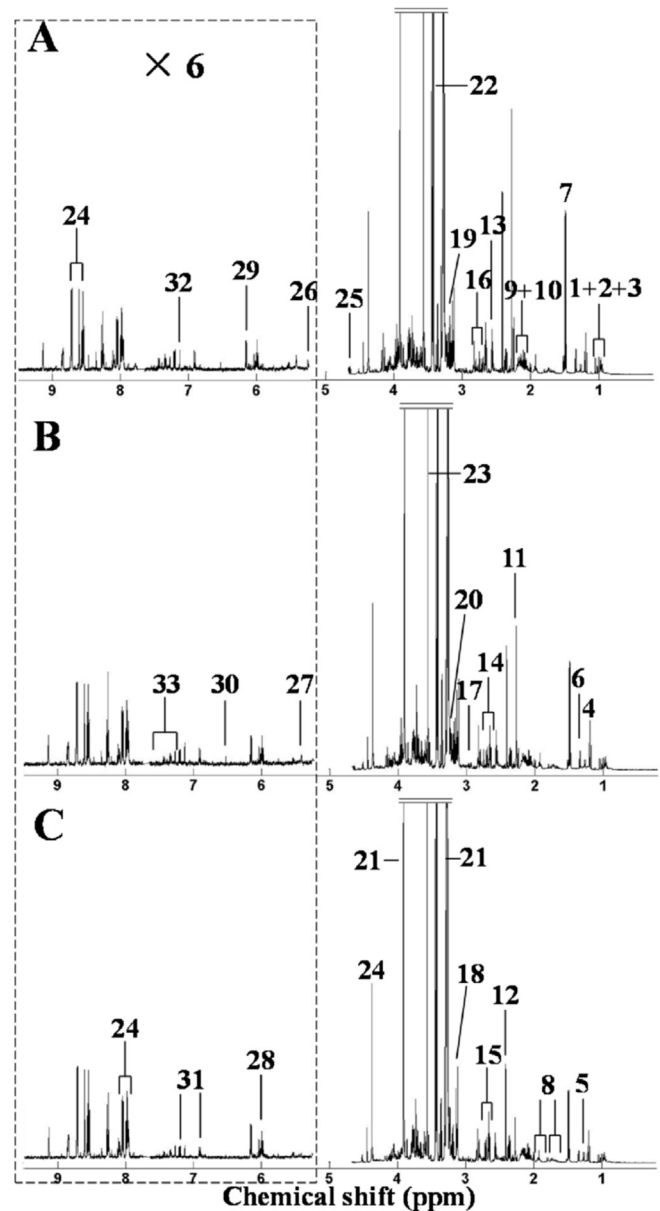

Fig. 3. Representative 1-dimensional ^{1}HNMR spectra of metabolite extracts from control (A), Cd- (B) and As (V)-treated (C) D-shape larval mussels *M. galloprovincialis*. **Keys**: (1) isoleucine, (2) leucine, (3) valine, (4) unknown 1 (1.20 ppm), (5) ethanol, (6) threonine, (7) alanine, (8) arginine, (9) glutamate, (10) glutamine, (11) acetoacetate, (12) succinate, (13) β-alanine, (14) hypotaurine, (15) aspartate, (16) asparagine, (17) dimethylglycine, (18) malonate, (19) choline, (20) phosphocholine, (21) betaine, (22) taurine, (23) glycine, (24) homarine, (25) β-glucose, (26) α-glucose, (27) glycogen, (28) unknown 2 (5.98 ppm), (29) ATP, (30) fumarate, (31) tyrosine, (32) histidine and (33) phenylalanine.

Decreased alanine may be related to the reduced anaerobic metabolism induced by Cd in D-shape larval mussels. In one possible metabolic pathway, aspartate may be converted into succinate with no detectable changes in other compounds under anoxic conditions in mollusk resulting in the decreased aspartate and increased succinate [38]. Therefore the increased aspartate and decreased succinate meant the reduced anaerobic metabolism in Cd-treated D-shape larval mussels, which was consistent with the decreased alanine. Acetoacetate is a ketone body synthesized from acetyl-coenzyme A as the end product of fatty acid metabolism. The depleted acetoacetate implied the reduced lipid metabolism in D-
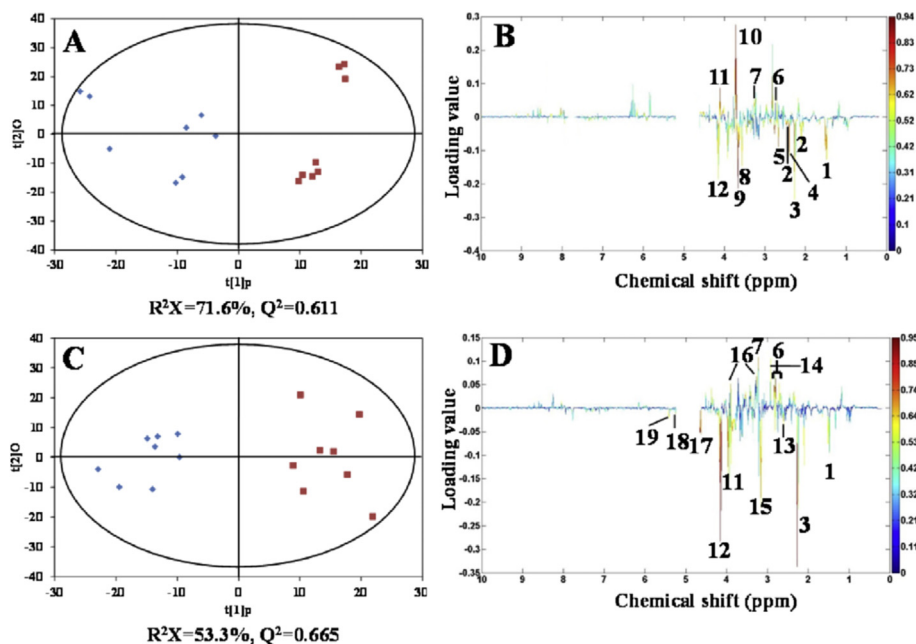
Fig. 4. OPLS-DA scores derived from ¹H NMR spectra of metabolite extracts from control (◆) and treatment groups (■) of D-shape larval mussels *M. galloprovincialis*, (A) Cd and (C) As (V), and corresponding coefficient plots (B) and (D). The color map shows the significance of metabolite variations between the two classes. Peaks in the positive direction indicate metabolites that are more abundant in treatment groups. Metabolites that are more abundant in the control group are presented as peaks in the negative direction. **Keys**: (1) alanine, (2) glutamine, (3) acetoacetate, (4) succinate, (5) hypotaurine, (6) aspartate, (7) phosphocholine, (8) glycine, (9) unknown 1 (3.67 ppm), (10) unknown 2 (3.73 ppm), (11) unknown 3 (3.95 ppm), (12) unknown 4 (4.15 ppm), (13) β-alanine, (14) dimethylglycine, (15) malonate, (16) betaine, (17) β-glucose and (18) α-glucose and (19) glycogen.

shape larval mussels. Choline and ATP can be catalyzed into phosphocholine and ADP by choline kinase, which is related to energy metabolism. The elevated phosphocholine suggested that Cd exposure enhanced the conversion of choline to phosphocholine in D-shape larval mussels.

For the As (V) treatment, alanine, acetoacetate, aspartate and phosphocholine, were similarly altered in D-shape larval mussels. These metabolic responses exhibited that As (V) induced disturbances in energy metabolism and osmotic regulation and reduced lipid metabolism in D-shape larval mussels compared with those in Cd-treated group. Although aspartate was increased in As (V)-treated samples, however, succinate was not significantly decreased, which suggested that the increased aspartate might be related to the disturbed osmotic regulation. The uniquely altered metabolites, including dimethylglycine, betaine, β-alanine, malonate, glucose and glycogen, indicated the differential biological effects of As (V) exposure, compared with those induced by Cd exposure in D-shape larval mussels. As two main osmolytes, dimethylglycine and betaine, were significantly elevated, indicating the obvious osmotic stress in D-shape larval mussels, together with the elevated amino acid, aspartate. Apparently, the altered dimethylglycine and betaine suggested that As (V) induced osmotic stress in D-shape larval mussels via different pathways compared with Cd. The two depleted amino acids, alanine and β-alanine, might be used to compensate the elevated dimethylglycine and betaine involved in osmotic regulation. Malonate is a competitive inhibitor of the enzyme succinate dehydrogenase that is involved in the Krebs cycle. Therefore, the decreased malonate suggest that As (V) influenced energy metabolism, while decreased glucose and glycogen indicated the mobilization of energy reserves induced by As (V) exposure in D-shape larval mussels.

In summary, the biological effects of the environmentally relevant concentration of Cd and As (V) were characterized in the early life stage (D-shape larvae) of mussels *M. galloprovincialis* using a combined proteomic and metabolomic approach. Basically,

proteomic responses indicated that Cd exposure induced obvious immune stress, oxidative stress, cellular injury and disturbance in nucleic acid metabolism in D-shape larval mussels. Interestingly, however, only two identified proteins were significantly altered in As (V)-treated group, which implied that D-shape larval mussel was less sensitive to As (V) than to Cd at protein level. These two proteins in response to As (V) exposure suggested As (V) influenced anti-oxidative system and cell proliferation in D-shape larval mussels. The metabolic responses indicated that Cd and As (V) induced clear disturbances in osmotic regulation and energy metabolism in D-shape larval mussels via different metabolic pathways. In addition, Cd reduced the lipid metabolism in D-shape larval mussels. This work demonstrated that a combination of proteomics and metabolomics could provide an insightful view in the biological effects of pollutants in mussel *M. galloprovincialis* at early life stage.

Acknowledgments

References

[1] J. Mu, The Evaluation of Ecological Environment for Key Fishery Waters in Bohai Sea (In Chinese). Master's thesis, Ocean University of China, 2009.
[2] W. Liu, W. Qiu, J. Chen, Distribution characteristics of trace pollutants in benthic mussels from the coastal areas of Bohai Sea and north Yellow Sea (In Chinese), Environ. Sci. 32 (2011) 445–451.
[3] C. Ji, D. Yu, Q. Wang, F. Li, J. Zhao, H. Wu, Impact of metal pollution on shrimp *Crangon affinis* by NMR-based metabolomics, Mar. Pollut. Bull. 106 (2016) 372–376.
[4] R. Chester, Marine Geochemistry, Allen & Unwin, Australia, 1990, p. 698.
[5] J.M. Neff, Ecotoxicology of arsenic in the marine environment, Environ. Toxicol. Chem. 16 (1997) 917–927.

[6] K. Bouilly, B. Gagnaire, M. Bonnard, H. Thomas-Guyon, T. Renault, P. Miramand, S. Lapègue, Effects of cadmium on aneuploidy and hemocyte parameters in the Pacific oyster, *Crassostrea gigas*, Aquat. Toxicol. 7 (2006) 149—156.

[7] M. Chang, W. Wang, A. Wang, T.T. Tian, P. Wang, Y. Zheng, Y. Liu, Effects of cadmium on respiratory burst, intracellular Ca^{2+} and DNA damage in the white shrimp Litopenaeus vannamei, Comp. Biochem. Physiol. Part C 149 (2009) 581—586.

[8] R. Company, A. Serafim, M.J. Bebianno, R. Cosson, B. Shillito, A. Fiala-Médioni, Effect of cadmium, copper and mercury on antioxidant enzyme activities and lipid peroxidation on the gills of the hydrothermal vent mussel *Bathymodiolus axoricus*, Mar. Environ. Res. 58 (2004) 377—381.

[9] T.D. Williams, N. Turan, A.M. Diab, H. Wu, C. Mackenzie, K.L. Bartie, O. Hrydziuszko, B.P. Lyons, G.D. Stentiford, J.M. Herbert, J.K. Abraham, I. Katsiadaki, M.J. Leaver, J.B. Taggart, S.G. George, M.R. Viant, K.J. Chipman, F. Falciani, Towards a system level understanding of non-model organisms sampled from the environment: a network biology approach, PLoS. Comput. Biol. 7 (2011) 1—20.

[10] M.R. Viant, E.S. Rosenblum, R.S. Tjeerdema, NMR-based metabolomics: a powerful approach for characterizing the effects of environmental stressors on organism health, Environ. Sci. Technol. 37 (2003) 4982—4989.

[11] Q. Song, H. Chen, Y. Li, H. Zhou, Q. Han, X. Diao, Toxicological effects of benzo(a)pyrene, DDT and their mixture on the green mussel *Perna viridis* revealed by proteomic and metabolomic approaches, Chemosphere 144 (2016) 214—224.

[12] Q. Song, P. Zheng, L. Qiu, X. Jiang, H. Zhao, H. Zhou, Q. Han, X. Diao, Toxic effects of male *Perna viridis* gonad exposed to BaP, DDT and their mixture: a metabolomic and proteomic study of the underlying mechanism, Toxicol. Lett. 240 (2016) 185—195.

[13] E.D. Goldberg, M. Koide, V. Hodge, A.R. Flegal, J. Martin, U.S. Mussel Watch, 1977—1978 results on trace metals and radionuclides, Estuar. Coast. Shelf Sci. 16 (1983) 69—93.

[14] M.H. Salazar, S.M. Salazar, Tributyltin Effects on Juvenile Mussel Growth. OCEANS'87, IEEE, 1987, pp. 1504—1510.

[15] H. Wu, A.D. Southam, A. Hines, M.R. Viant, High-throughput tissue extraction protocol for NMR- and MS-based metabolomics, Anal. Biochem. 372 (2008) 204—212.

[16] P.A. Kirkland, J. Busby, S. Stevens Jr., J.A. Maupin-Furlow, Trizol-based method for sample preparation and isoelectric focusing of halophilic proteins, Anal. Biochem. 351 (2006) 254—259.

[17] F.W.-F. Lee, S.C.-L. Lo, The use of Trizol reagent (phenol/guanidine isothiocyanate) for producing high quality two-dimensional gel electrophoretograms (2-DE) of dinoflagellates, J. Microbiol. Meth. 73 (2008) 26—32.

[18] C. Ji, H. Wu, L. Wei, J. Zhao, J. Yu, Proteomic and metabolomic analysis reveal gender-specific responses of mussel *Mytilus galloprovincialis* to 2,2',4,4'-tetrabromodiphenyl ether (BDE 47), Aquat. Toxicol. 140—141 (2013) 449—457.

[19] E. Mortz, T.N. Krogh, H. Vorum, A. Gorg, Improved silver staining protocols for high sensitivity protein identification using matrix-assisted laser desorption/ionization-time of flight analysis, Proteomics 1 (2001) 1359—1363.

[20] F. Gharahdaghi, C.R. Weinberg, D.A. Meagher, S.M. Mische, Mass spectrometric identification of proteins from silver-stained polyacrylamide gel: a method for the removal of silver ions to enhance sensitivity, Electrophoresis 20 (1999) 601—605.

[21] H. Katayama, T. Nagasu, Y. Oda, Improvement of in-gel digestion protocol for peptide mass fingerprinting by matrix-assisted laser desorption/ionization time-of-flight mass spectrometry, Rapid Commun. Mass Spectrom. 15 (2001) 1416—1421.

[22] A. Shevchenko, M. Wilm, O. Vorm, M. Mann, Mass spectrometric sequencing of proteins from silver-stained polyacrylamide gels, Anal. Chem. 68 (1996) 850—858.

[23] Y. Gachet, S. Tournier, M. Lee, A. Lazaris-Karatzas, T. Poulton, U.A. Bommer, The growth-related, translationally controlled protein P23 has properties of atubulin binding protein and associates transiently with microtubules during the cell cycle, J. Cell Sci. 112 (1999) 1257—1271.

[24] J.L. Stark, K. Mehla, N. Chaika, T.B. Acton, R. Xiao, P.K. Singh, G.T. Montelione, R. Powers, Structure and function of human DnaJ homologue subfamily a member 1 (DNAJA1) and its relationship to pancreatic cancer, Biochemistry 53 (2014) 1360—1372.

[25] S. Mkrtchian, M. Baryshev, O. Matvijenko, A. Sharipo, T. Sandalova, G. Schneider, M. Ingelman-Sundberg, Oligomerization properties of ERp29, an endoplasmic reticulum stress protein, FEBS Lett. 431 (1998) 322—326.

[26] W. Zhang, Q. Wei, Calcineurin stimulates the expression of inflammatory factors in RAW 264.7 cells by interacting with proteasome subunit alpha type 6, Biochem. Biophys. Res. Commun. 407 (2011) 668—673.

[27] N. He, H. Liu, X. Xu, Identification of genes involved in the response of haemocytes of Penaeus japonicus by suppression subtractive hybridization (SSH) following microbial challenge, Fish. Shellfish Immunol. 17 (2004) 121—128.

[28] H. Wu, C. Ji, L. Wei, J. Zhao, H. Lu, Proteomic and metabolomic responses in hepatopancreas of *Mytilus galloprovincialis* challenged by *Micrococcus luteus* and *Vibrio anguillarum*, J. Proteom. 94 (2013) 54—67.

[29] E.H. Sarsour, A.L. Kalen, P.C. Goswami, Manganese superoxide dismutase regulates a redox cycle within the cell cycle, Antioxid. Redox Signal 20 (2014) 1618—1627.

[30] E. Abele, E. Philip, P.M. Gonzalez, S. Puntarulo, Marine invertebrate mitochondria and oxidative stress, Front. Biosci. 12 (2007) 933—946.

[31] C. Ji, H. Wu, L. Wei, J. Zhao, iTRAQ-based quantitative proteomic analyses on the gender-specific responses in mussel *Mytilus galloprovincialis* to tetrabromobisphenol A, Aquat. Toxicol. 157 (2014) 30—40.

[32] N. Hirokawa, Kinesin and dynein superfamily proteins and the mechanism of organelle transport, Science 279 (1998) 519—526.

[33] A. Kornberg, On the metabolic significance of phosphorolytic and pyrophosphorolytic reactions, in: Horizons in Biochemistry, 1962, pp. 251—264.

[34] Y.K. Ghiorghi, K.I. Zeller, C.V. Dang, P.A. Kaminski, The c-Myc target gene Rcl (C6orf108) encodes a novel enzyme, deoxynucleoside 5'-monophosphate N-glycosidase, J. Biol. Chem. 282 (2007) 8150—8156.

[35] R. Company, O. Antúnez, M.J. Bebianno, M.P. Cajaraville, A. Torreblanca, 2-D difference gel electrophoresis approach to assess protein expression profiles in *Bathymodiolus azoricus* from Mid-Atlantic Ridge hydrothermal vents, J. Proteom. 74 (2011) 2909—2919.

[36] Y. Sasagawa, Y. Urano, Y. Kohara, H. Takahashi, A. Higashitani, *Caenorhabditis elegans* RBX1 is essential for meiosis, mitotic chromosomal condensation and segregation, and cytokinesis, Genes Cells 8 (2003) 857—872.

[37] T.M. Stokes, J. Awapara, Alanine and succinate as end-products of glucose degradation in the clam *Rangia cuneata*, Comp. Biochem. Physiol. 25 (1968) 883—892.

[38] R.A. Graham, W.R. Ellington, Anaerobic aspartate metabolism and the formation of alanine in molluscan cardiac muscle: a ^{13}C NMR study, J. Exp. Zool. 236 (1985) 365—370.